Nature Environment and Pollution Technology
An International Quarterly Scientific Journal

p-ISSN: 0972-6268
(Print copies up to 2016)
e-ISSN: 2395-3454

Vol. 20 | No.4 | pp. 1789-1801 | 2021

Original Research Paper

https://doi.org/10.46488/NEPT.2021.v20i04.045

Open Access Journal

A GIS-Based Methodology to Determine Effect of Vehicular Pollution at Ward Level: Case Study of Jaipur City

A. D. Vyas*†, K. Mahale* and R. Goyal**
*Department of Civil Engineering, Manipal University Jaipur, India
**Department of Civil Engineering, Malaviya National Institute of Technology, Jaipur, India

Nat. Env. & Poll. Tech.
Website: www.neptjournal.com

Received: 09-11-2020
Revised: 26-01-2021
Accepted: 20-02-2021

Key Words:
Air pollution
Linear regression
NO_2
Road density

ABSTRACT

To determine appropriate measures to reduce air pollution in any urban city, the first essential requirement is to estimate the spatial distribution of air pollution parameters in that area. In absence of air monitoring stations, alternative methods are required for the same. In the present work, a GIS-based methodology is presented to estimate the level of NO_2 based on the road density of the road network of different categories of roads. Road network GIS layer and measured levels of the average value of NO_2 for the year 2019 at 12 air pollution monitoring stations of Jaipur city are used to develop a large number of possible linear regression models for estimation of NO_2 values based on road density values. Akaike Information Criterion (AIC) and adjusted r^2 values are used to evaluate and arrive at the best-fitted model. Values from the cities of Jodhpur and Kota are used to validate the model. Using this model, NO_2 levels are determined at 91 wards of Jaipur city and the output is compared with the similar map derived based on interpolation of NO_2 values at the 12 monitoring stations. It is concluded that the methodology developed in this study generates better estimates of NO_2 at the ward levels.

INTRODUCTION

Climate change due to global warming is the major crisis, presently the world is facing. Climate change is closely related to the rise in air pollution. As per Institute for Advanced Sustainability Studies (IASS 2020), these air pollutants are responsible for climate change by affecting the incoming solar radiation. Few pollutants find their way and are absorbed by the atmosphere whereas others are reflected by the atmosphere thereby affecting the earth's atmosphere by cooling or warming it. Ground-level ozone, methane, and black carbons are classified under short-lived climate-forcing pollutants (SLCPs). A report by World Health Organization (2019) predicts that air pollutants are the biggest reason for the major health threat and severely affecting climatic conditions. As per the latest report by Health Effects Institute (2020 a), air pollution is the major cause of 1 in 9 deaths globally. It has been estimated that globally 6.67 million mortalities in the year 2019 were because of air pollution. This is majorly attributed to smog in the outer atmosphere and smoke inside the homes. Heart diseases, strokes, chronic obstructive pulmonary diseases resulting from acute respiratory infections, cancer of the lungs are major contributors to high mortality rates. It is estimated that nine out of ten people are inhaling polluted air with higher levels. UNICEF (2016) press report projected that 300 million children are breathing toxic air. As per the United States Environmental Protection Agency (2020), particulate matter affects the lungs and heart which is also confirmed through numerous scientific studies across the globe. The United States Environmental Protection Agency (2016) has identified six "criteria" air pollutants as these pollutants are regulated under environmental and human health-based criteria by the Center for Disease Control and Prevention (CDC 2019). These pollutants are CO, NO_2, SO_2, particulate matter, ground-level ozone, and lead. It is mentioned that not enough data may be available on the effects of air pollutants on the health of human beings, still, it is considered a major risk multiplier for the health of human being specially in developing countries. The latest findings on air pollutant impacts on human health as published in the Lancet, "Global Burden of Disease" is very alarming for a country like India. Indeed, Indian population has the maximum exposure to PM 2.5 and the third highest exposure to O_3. It is estimated that almost 1.67 million deaths annually are caused in India due to air pollutants which include 116,000 infants as reported in State of Global Air 2020, Health Effects Institute (2020b).

A study done for natural aerosols in South Gobi Desert by Filonchyk & Hurynovich (2020) was found to be of great importance. Data from 2016 to 2019 was analyzed to find the spatial-temporal patterns of atmospheric pollutants in eight cities. It was reported that occurrence rates of pollutants exceeding in concentrations with respect to the

Chinese National Ambient Air Quality Standard (CNAAQS) grade 1 and grade 2 were 40.1% and 5.4% for $PM_{2.5}$ and 82.9% and 11.64% for PM_{10} in the region. Khaniabadi et al. (2020) studied the impact on health due to an increase in the concentration of different pollutants by 10 $\mu g.m^{-3}$. They studied the effect of PM_{10}, NO_2, and O_3 in Kermanshah City, Iran. The results indicated that a $\mu g.m^{-3}$ change in PM_{10}, NO_2, and O_3 increases the relative risk by 1.066, 1.012, and 1.020, respectively.

Remote sensing has proved to be useful for depicting spatial variability of air pollutants in an urban area (Bechle et al. 2013). In their study, estimates of surface NO_2 levels recorded by Ozone Monitoring Instrument (OMI) onboard NASA's Aura satellite were compared with values recorded by US EPA ambient monitoring stations. OMI measures the daily level of NO_2 tropospheric column abundance. Scaling factors (surface-to-column ratios) were used to relate satellite data to ground-level measurements. Costabile et al. (2010) studied the distribution of pollutants NO_x, SO_2, NO_2, Xylenes, Benzene, and Toluene within the urban area of Lanzhou, China to understand the spatial distribution of these pollutants. The investigation found that it was mainly governed by the factors responsible for the diffusion of emission sources through space.

Nieto et al. (2015) collected levels of CO, PM_{10}, NO_x, O_3, and SO_2, for 3 years to build a regression model of air quality for the urban area of Oviedo, Spain. The model was built at a local scale using a multivariate adaptive regression splines (MARS) technique. Mohammad and Juahir (2015) identified the spatial pattern of air pollutants in the northern part of Peninsular Malaysia. The study was carried out from 2008 to 2011, covering seven air pollution monitoring stations. The main pollutants that were part of the study were NO_2, O_3, CO, and PM_{10} obtained from the Department of Environment, Malaysia (DoEM). ANOVA, Artificial Neural Network (ANN) and environ metric techniques (HACA and Descriptive Analysis approaches) were used in analyzing the data. They reported that based on ANOVA single test, the *p*-value of PM_{10} is significantly a smaller alpha level (p=0.05) and is therefore suitable for further analysis as compared to O_3, NO_2, and CO.

Ryu et al. (2019) used the GIS-based kriging interpolation method to develop a nationwide map of NO_2 concentration over South Korea. Remote sensing data was integrated with the ground observations and a good value of root-mean-square standardized (RMSS) error was obtained. In their study, they compared data for different data sources which include detailed national data besides remote sensing data and other sources. In the study, it was reported that the average concentration was highest when data was taken through remote sensing. LUR models that are land-use regression models were formulated to analyze the concentration of NO2 in both urban and non-urban areas. In their paper, Zhu & Lok (2018) described the temporal and spatial variability of nitrogen dioxide concentrations at the level of major streets for densely populated parts of Hong Kong with very high traffic volumes. Using a combination of remote sensing data and direct measurement in the field, temporal variations were differentiated with spatial distributions. This was carried out by ignoring the flow pattern of traffic and concentrating on changes in the spatial distribution of NO_2.

Walkability one of the measure for air pollutants pertaining to traffic was defined by Cowie et al. (2016). They compared walkability with weighted road density for Sydney neighborhoods, representing 3.6 million population. High walkability and low weighted road density were defined as "sweet spots" and reverse of that as "sour spots" in the neighborhoods. Even short exposure to a higher concentration of NO_2 can aggravate asthma, respiratory diseases and even visiting hospital emergency rooms (EPA, 2016). In a report by the United States Environmental Protection Agency, (2016), it was reported that a long duration exposure of NO_2 severely affected children and elderly citizens. In the atmosphere, NO_2 and NO_x react with other chemicals to form ozone and particulate matter which when inhaled are disastrous to human health, mainly affecting the respiratory systems. Carslaw et al. (2019) in their report raised concern over the exceeding concentrations of NO_2 of more than 40 $\mu g\ m^{-3}$ as prescribed by the European Directive limit value. Munoth et al. (2015) reported higher levels of NO_2 and Fluoride in groundwater in Rajasthan state.

Nitrogen dioxide (NO_2) which is mainly emitted from vehicular emissions is yellow-brownish in color is also emitted from industrial activity and power plants. As per the Hindu (2015), the emission of gas has reached significantly high in India and South Asia region during the decade 2005-14 as projected in a study through NASA satellite map. NASA satellite maps predict that exposures of Nitrogen dioxide even for short periods can aggravate respiratory diseases, asthma and can also lead to hospitalizations.

Balakrishnan et al. (2019) discussed that though cardiovascular diseases are the largest cause of death in India but are closely followed by air pollution, which is the second largest reason for premature deaths in India. Till the 1990s, air pollution was relatively lower in the list of causes that caused most deaths in India. In another study, it has been reported that Rajasthan is amongst the leading states in the country with the widespread cause of chronic obstructive pulmonary disease (COPD) (TNN 2017) and asthma induced deaths which in turn is linked to air pollution in more than

half the cases followed by smoking for a quarter of the cases. According to ORGCC (2020), approximately one-third percent of the children in Jaipur suffer from acute respiratory infection (ARI). It was further emphasized that the figure has been increasing recently. Overall, in Jaipur, there has been an increase in Rhinitis, asthma, bronchitis, pneumonia, COPD, chronic cough, sneezing, itching, eye problems ARI, and other respiratory issues. Rajasthan tops the list when it comes to deaths due to air pollution, according to Singh (2019). Using geostatistical and geospatial techniques Dadhich et al. (2018b) estimated the temporal and seasonal variations (2004–2015) of particulate and gaseous pollutants in the city of Jaipur. They performed an ordinary least square (OLS) regression technique to reveal a good correlation between Air Quality Index and weathering features like wind speed, humidity, and temperature for both winter and summer seasons. Similarly, Dadhich et al. (2018a) also used GIS-based approaches for assessing the ambient air quality standards of Kota city.

To reduce the impact of air quality parameters in any area, the first essential requirement is to estimate the spatial distribution of these parameters in that area. This would provide an indication of areas where the air quality is bad or lower than the standard. If this information is available, it becomes easier for urban planners and experts to apply remedial measures and subsequent actions can be taken in the areas which are highly polluted. Adequate measurements thus can be planned and taken in those areas. Estimate of air quality parameters in any area is typically determined with the help of observed values of these parameters at air quality monitoring stations. Different interpolation tools are used to predict the values at other places. However, the density of such air quality monitoring stations is presently extremely too low in many urban areas. Determining air quality in such areas, other than the vicinity of such sensors, is a challenging task. Interpolation typically leads to extrapolation as monitoring stations are usually located in the central part of the city. This leads to the overestimation of air pollution parameters in the urban periphery of big cities. Therefore, a methodology is desired which could estimate the air quality parameter even in the absence of monitoring stations.

In the present study, a new methodology is presented which determines the value of NO_2 due to vehicular pollution, based on the density of the road network of any area. The road network layer, consisting of roads of different categories, such as highways, major roads, and inner roads, of any urban area, can easily be mapped using various remote sensing systems or google earth. Such road network layers could be generated and updated on regular basis. Therefore, a methodology that is dependent on such easily available information is likely to be of great importance in the absence of a good density of air quality monitoring stations.

Jaipur city with almost 3.5 million urban population as of 2020 (3.1 million as per 2011 census) has three continuous monitoring stations named Continuous Ambient Air Quality Monitoring Stations (CAAQMS) and nine manual stations. Pollutants emitted from vehicular emissions like Nitrogen Dioxide (NO2) and particulate matter PM10 are key pollutants that are continuously monitored at these stations besides other pollutants. The data available is of very limited capacity for a large area of 470 sq km of Jaipur city. Even if it is required to find out the concentration at ward level from these 12 points through GIS spatial interpolation methods, the density is not appropriate, and therefore data is rather extrapolated or interpolated between drastically different points locations. In that case, the values are likely to be not accurate except for those wards where these stations are located. In this paper, there has been an attempt to relate Jaipur road network layer data with available vehicular pollutant data (NO_2) measured at 12 air pollution monitoring stations. A large number of possible models are generated, and their prediction accuracy is compared between different models. Multi-model selection criteria such as the Akaike information criterion and Bayesian information criterion are used to select better-performing models amongst the several hundred models generated. Model output for two additional air quality monitoring stations of Jodhpur and Kota cities are used to validate the model. Estimated values of NO_2 are determined for all the wards of Jaipur city to understand the spatial distribution of vehicular pollution in Jaipur city.

STUDY AREA

Jaipur the capital city of Rajasthan state is a big tourist hub; part of the golden triangle is also called as pink city of India. As per the 2011 census, Jaipur has a population of around 3.1 million which is characterized by high summer temperatures, low rainfalls, and mild winter as shown in Fig. 1. The average yearly rain for the city is just below 600 mm in comparison to India's national average of almost 1100 mm. The city recorded a yearly growth rate of five percent in 2011 in comparison to 2001 and was ranked 10^{th} among India's megacities (Sogani & Vyas 2019). The city is part of the government of India's Smart City Program and there are massive plans for urban infrastructure development. The maps of zones and wards of the city are as per JDA (2020) and were further digitized. Fig. 1 shows the different zones and wards of Jaipur city. Table 1 gives major information about the city.

All the 91 wards of Jaipur city based on 2019 classifications were taken into consideration for this study (Vyas

Table 1: Key statistics of Jaipur City

Study area: Name of city	Jaipur City	
Total Area	467 Square Kilometres	
City Wards and Zones	91 wards and 8 zones	
Total House Holds	737179	
Total Population covered	3046185 (As per the year 2011 census data)	
	Male	1603136
	Female	1443048
	Sex Ratio	900 Females per 1000 Males

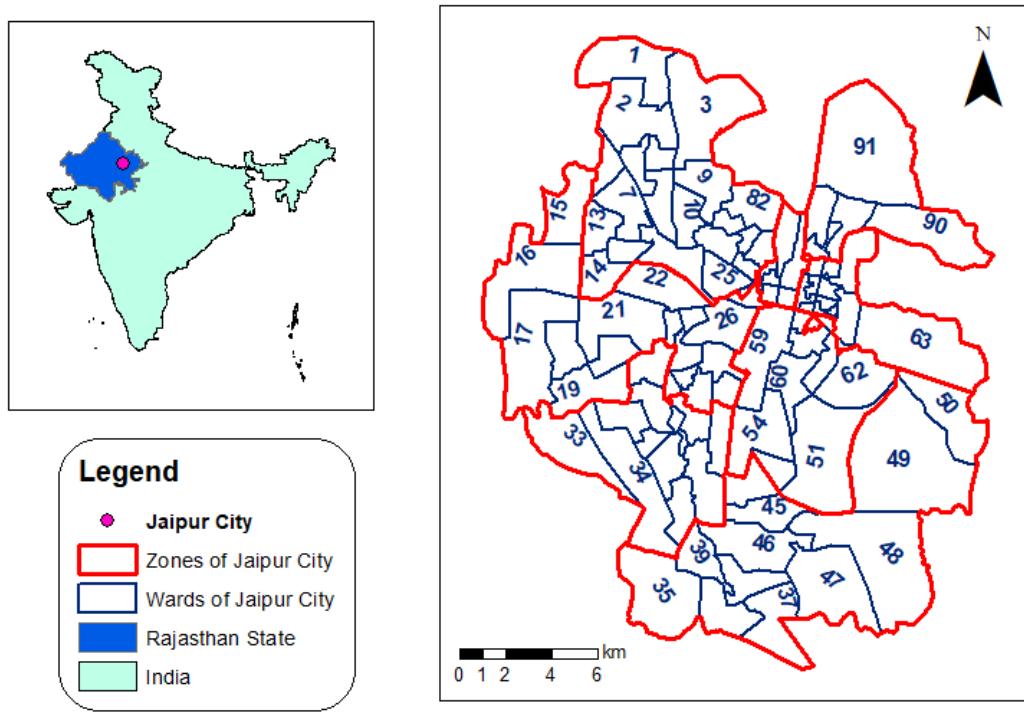

Fig. 1: Zones and wards of Jaipur city.

et al, 2020a). A new bifurcation of city wards was done in December 2019 where the city wards were reclassified into a total of 250 wards. The Greater Jaipur has 150 wards and Heritage Jaipur has 100 wards. This study was confined to 8 Zones and 91 wards as shown in Table 2**.**

Ambient air quality is continuously monitored in the city as State Pollution Control Board has installed three Continuous Ambient Air Quality Monitoring Station (CAAQMS) and nine manual air quality monitoring stations under National Air Quality Monitoring Programme (NAMP), as shown in Fig 2. At CAAQMS Particulate Matter ($PM_{2.5}$ and PM_{10}), Gaseous pollutants, NO_x, SO_2, CO, O_3 VOC, and NH_3, and Meteorological parameters like Wind Speed, Wind Direction, Temperature, Relative Humidity, Solar Radiation, Pressure, etc. are measured continuously (Vyas et al. 2020). At NAMP stations PM_{10}, NO_2, and SO_2 are measured twice a week. Due to the dry conditions prevailing over a major part of the year, levels of PM10 are found to be in excess. Suspended particulate matter coming from road dust, construction and demolition activities, vehicular emissions, burning of fossil fuels, and solid waste in open, industrial emissions are key air pollutants of the city.

Table 3 shows the annual average PM_{10} and NO_2 values at different stations for the year 2019. Fig. 3 and Fig. 4 show

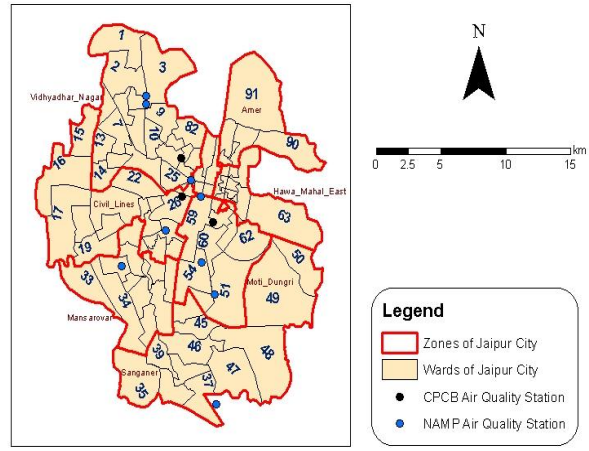

Fig. 2: Location of air quality monitoring stations.

Table 2: Classification of Jaipur city Wards and Zones

S. No.	Name of Zone	Total Wards	Classification of Wards
1	Vidhya Dhar Nagar	21	1 to 14, 23 to 25 and 79-82
2	Civil Lines	16	15 to 22, 26 to 28, 30, 56 to 58 and76
3	Man Sarovar	11	29, 31 to 34, 40 to 44 and 55
4	Sanganer	12	35 to 39, 45 to 50 and 52
5	Moti Doongri	9	51, 53 and 54, 59 to 62, 64 and 65
6	Hawa Mahal East	11	63 to 73, 85 and 86
7	Hawa Mahal West	6	74 and 75, 77 and 78, 83 and 84
8	Amer	5	87 to 91

the spatial distribution of PM_{10} and NO_2 concentrations for the year 2019 for Jaipur city based on the annual average observed values of these parameters at the monitoring stations. As can be seen, most of the variation is visible only in the closed proximity of the air quality monitoring stations. Since monitoring stations only exist inside the city area,

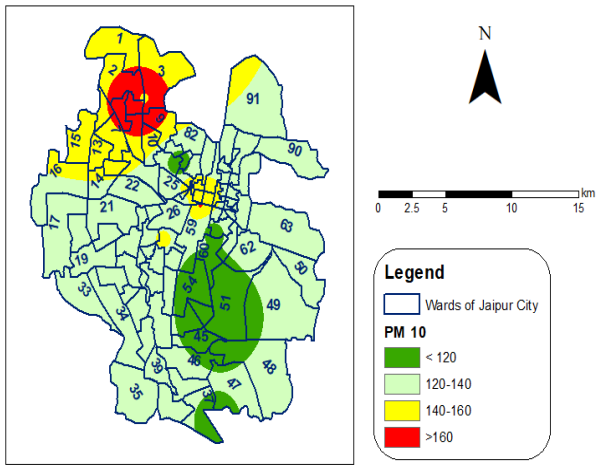

Fig. 3: Spatial distribution of average annual PM_{10}.

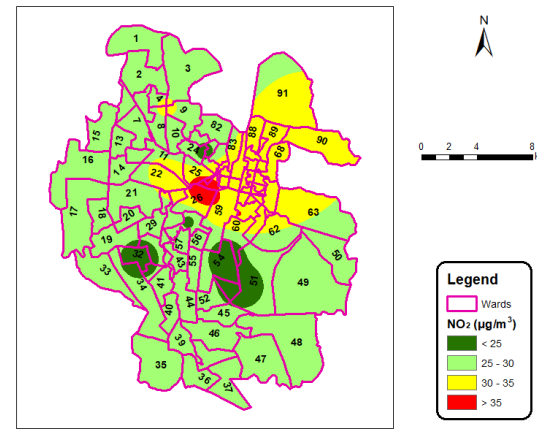

Fig. 4: Spatial distribution of average annual NO_2.

Table 3: Air Quality Parameters of Year 2019

Station Code	Latitude	Longitude	NO_2 (µg/m^3)	PM_{10} (µg/m^3)
101	26.974	75.774	31.41	193.21
102	26.927	75.809	34.21	150.80
103	26.876	75.817	21.41	102.95
104	26.855	75.827	23.36	108.99
105	26.873	75.754	23.64	127.62
106	26.896	75.788	24.30	141.94
107	26.787	75.827	27.46	119.56
108	26.979	75.774	27.00	160.00
109	26.916	75.816	33.80	163.34
110	26.901	75.825	35.08	100.87
111	26.916	75.801	43.15	127.26
112	26.940	75.801	22.57	116.09

where traffic density and hence air pollution parameter levels are generally high, when interpolation is used, most of the outskirts of Jaipur city also show high levels of NO_2 values. NO_2 levels are likely to be lesser in these areas as the traffic density, a major contributor of NO_2 is much less as compared to inner city areas.

From the interpolated maps and using the zonal statistics tool, the average concentration of PM_{10} and NO_2 could also be derived at the ward level. Color-coded maps are then plotted showing levels of PM_{10} and NO_2 for different wards (Fig. 5 and 6). Most of the outer area of Jaipur city is classified under the category of 25-30 for NO_2, which seems to be on the higher side as traffic in these areas is typically lower than in the city area.

All roads of Jaipur cities were classified into three different groups based on estimated traffic on these roads. Level 01 roads are those roads that carry most of the daily vehicular traffic of the city. Level 02 roads are those interconnecting level 01 roads. Though traffic on these roads is less than the level 01 roads however it is still good enough to generate some level of vehicular pollution. Level 03 roads are inner roads, typically carrying only the vehicular traffic of residents of that area. Though the level of pollution may be less on these roads, however, their density is more than that of other levels of roads. It is also observed that typically inner roads have a better level of plantations around the roads as compared to level 01 and 02 roads. Due to this, these roads may be serving as a sink for NO_2 pollution rather than the generation of pollution. Fig. 7 shows all the three levels of roads in sub maps A, B, and C respectively.

MATERIALS AND METHODS

Road maps of any area could be used to generate road density maps at different search radius levels. The line density tool

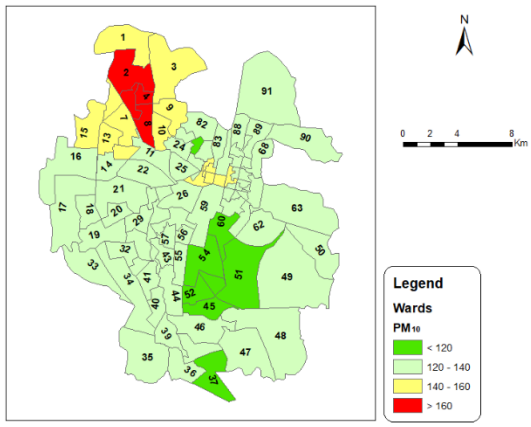

Fig. 5: Ward-wise levels of average PM_{10}.

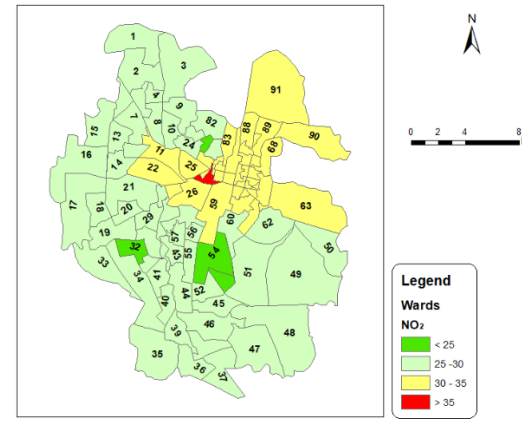

Fig. 6: Ward-wise levels of average NO_2.

calculates the density of linear features in the neighborhood of each output raster cell. Road density is determined in m length per m^2 area within the search radius. Conceptually, a circle of the size of the search radius is drawn around each raster cell center. The length of the portion of each road that falls within the circle is calculated. These figures are summed for all the roads falling within the search radius and the total is divided by the circle's area. Road density maps of different levels were generated for different search radius of 125, 250, 500, 750, 1000, 1250, and 1500 m. Fig. 8 shows the road density map of level 01 roads for the search radius of 750 m. Further buffer tool of GIS was used to generate planar buffers of the same sizes, as the search radius used for road density calculation, around each of the monitoring station. So, planar buffers of sizes 125, 250, 500, 750, 1000, 1250, and 1500 m were generated around each monitoring station. A dissolved type of none was used to ensure that each monitoring station has its own buffer even in case of partial overlap of buffers of different stations. Fig. 9 shows the buffers of 500m for all monitoring stations.

Using the buffer maps (Arc Map 2020a, 2020b) of a particular radius, say 1000 m, and road density maps of the same search radius of 1000 m, the zonal statistics tool was used to calculate the mean value of road density around each individual station for different road levels with different search radius.

Table 4 shows the value of road densities for all three levels of the road network around each monitoring station for a search radius of 750 and 1000 m.

RESULTS AND DISCUSSION

A large number of linear regression models could be developed to find the relationship between air pollution parameters PM_{10} or NO_2 or a combination of them with the road density values of different levels of roads for different search radius and buffer areas. For examples if RD_{Li}^{SRm} is Road density of road level i and search radius m then some models that could be tried are shown as eqns. 1, 2, 3, and 4 below.

$$NO_2 = f(RD_{L1}^{SR750}, RD_{L2}^{SR750}, RD_{L3}^{SR750}) \quad (1)$$

$$NO_2 = f(RD_{L1}^{SR1000}, RD_{L2}^{SR1000}) \quad (2)$$

$$PM_{10} = f(RD_{L1}^{SR1000}) \quad (3)$$

$$\log(NO_2) = f\left(\log(RD_{L1}^{SR750}, RD_{L2}^{SR750}, RD_{L3}^{SR750})\right) \quad (4)$$

A large number of combinations of different road levels and search radius could be taken as independent variables to find the relationship of them with dependent variables of air pollution parameters. Further variations such as linear and log-log combinations could be tried.

A total number of 192 different models were tried using a script developed in R language, out of which 96 models were using normal values of road density and air pollution parameters and 96 of them using $\log_{10}$ values of all parameters. Models with $\log_e$ (ln) were also tried, but they were giving poor results as compared to models with $\log_{10}$ and hence are not discussed further. To compare various models and to select which model is performing better, the coefficient of determination (r^2) is calculated for each model and com-

Table 4: Road Density Values Around Monitoring Stations

Station Code	Search Radius: 750 m			Search Radius: 1000 m		
	Level 01	Level 02	Level 03	Level 01	Level 02	Level 03
101	2.23	2.59	16.88	1.99	2.76	17.14
102	1.90	4.40	15.18	2.01	4.06	14.17
103	1.46	1.71	10.97	1.50	1.68	10.77
104	1.09	2.14	10.92	0.93	1.93	10.75
105	2.23	2.83	20.49	1.91	2.80	20.45
106	1.52	3.76	18.82	1.54	3.67	18.47
107	2.12	1.29	11.47	1.76	1.40	11.53
108	1.77	3.22	17.11	1.63	3.19	16.72
109	2.77	3.32	9.33	2.63	3.21	10.22
110	2.18	5.00	12.69	2.14	4.56	12.32
111	3.28	3.53	10.43	2.98	3.48	10.68
112	1.61	3.77	18.79	1.49	3.44	17.15

pared. r^2 is a scale-invariant statistic that gives the proportion of variation in the target variable explained by the linear regression model (Analytics Vidya 2020). The R-squared statistic suffers from a major flaw. Its value never decreases no matter the number of variables we add to our regression model, even if redundant variables are added. Therefore "Adjusted r^2" (referred to as adj r^2) values are determined. The adj r^2 takes into account the number of independent variables used for predicting the target variable.

It is well known that when fitting linear regression models between two sets of known and unknown variables, more than one model could be developed with almost comparing values of r^2 or adj r^2. Choosing a specific model between them would require evaluations of uncertainties associated with these models. A number of statistical criteria could be used to evaluate alternative models (Poeter & Anderson 2005). Akaike Information Criterion (AIC) and Bayesian Information Criterion (BIC) are used in the present work (Zhou & Herath 2017, Rajput et al. 2020).

AIC for a model could be calculated using eqns. 5, 6 and 7

$$AIC = n \ln(\sigma^2) + 2k \tag{5}$$

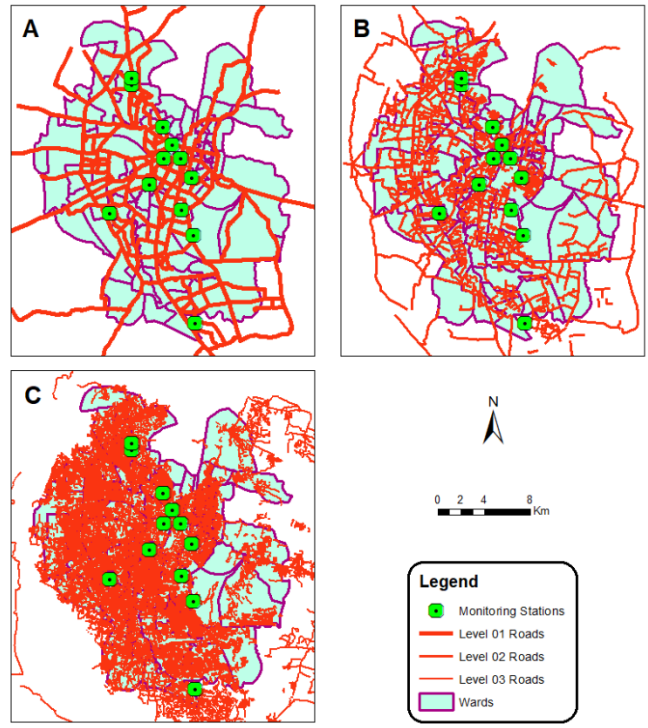

Fig. 7: Road maps of Jaipur city (A – Level 01, B – Level 02 and C – Level 03).

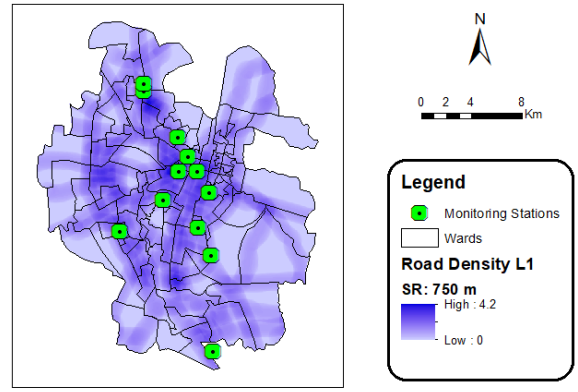

Fig. 8: Road density map of level 01 roads with search radius: 750 m.

$$\sigma^2 = \frac{SWSR}{n} \quad (6)$$

$$SWSR = \sum_{i=1}^{n} \omega_i [y_i - y_i'(b)]^2 \quad (7)$$

here:
n: number of observations, equal to 12 for all the models;
k: number of model parameters, varies from 1 to 3;
σ^2: residual variance;
SWSR: sum of weighted squared residuals;
ω_i: weight for the i^{th} observation, taken as 1 for all observations;
y_i, y_i': measured and model calculated dependent variable, respectively.

BIC is calculated as given in eqn. 8.

$$BIC = n \ln(\sigma^2) + k\, ln(n) \quad (8)$$

AIC and BIC values of all models were also evaluated using a script in R language. The model with minimum values of AIC was selected as the best model.

Models were divided into two different streams, one with normal values and another with $\log_{10}$ values of parameters. Table 5 shows the 5 best models of both the streams with the values of r^2, adj r^2, AIC, and BIC.

As can be seen, the best values of r^2 and adj r^2 are achieved for model 1, belonging to stream 1 of the models, which is between normal values of NO_2 and road density values of levels 1, 2, and 3 roads with a search radius of 750m. This model also gives the lowest AIC and BIC values in stream 1 of the models. In stream 2, the best model is model 6, which is for the same NO_2 and road density values of levels 1, 2, and 3 roads with a search radius of 750m, however with $\log_{10}$ values of all these parameters. This model gives lower r^2

Table 5: Performance parameters of different parameters

Model number	Stream 1: Normal values of parameters					
	Model description	r^2	adj r^2	AIC	BIC	p_m
1	$NO_2 = f(RD_{L1}^{SR750}, RD_{L2}^{SR750}, RD_{L3}^{SR750})$	0.86	0.81	64.47	66.90	42.6
2	$NO_2 = f(RD_{L1}^{SR1000}, RD_{L2}^{SR1000}, RD_{L3}^{SR1000})$	0.85	0.80	65.20	67.62	28.1
3	$NO_2 = f(RD_{L1}^{SR500}, RD_{L2}^{SR500}, RD_{L3}^{SR500})$	0.83	0.77	66.84	69.27	10.4
4	$NO_2 = f(RD_{L1}^{SR1000})$	0.76	0.74	67.17	68.62	10.0
5	$NO_2 = f(RD_{L1}^{SR1250}, RD_{L3}^{SR1250})$	0.80	0.75	67.18	69.12	8.9
	Stream 2: $\log_{10}$ values of parameters					
6	$\log(NO_2) = f(\log values\ of\ RD_{L1}^{SR750}, RD_{L2}^{SR750}, RD_{L3}^{SR750})$	0.81	0.74	-33.58	-31.16	39.7
7	$\log(NO_2) = f(\log values\ of\ RD_{L1}^{SR1000}, RD_{L2}^{SR1000}, RD_{L3}^{SR1000})$	0.80	0.72	-32.75	-30.32	27.6
8	$\log(NO_2) = f(\log values\ of\ RD_{L1}^{SR1000}, RD_{L3}^{SR1000})$	0.72	0.66	-30.76	-28.82	12.1
9	$\log(NO_2) = f(\log values\ of\ RD_{L1}^{SR500}, RD_{L2}^{SR500}, RD_{L3}^{SR500})$	0.76	0.67	-30.68	-28.25	10.3
10	$\log(NO_2) = f(\log values\ of\ RD_{L1}^{SR1000})$	0.66	0.63	-30.45	-29.00	10.2

and adj r^2 values, however, AIC and BIC values are negative values and much lower as compared to model 1. Based on adj r^2 values, it can be said that model 1 explains 81% of the variations in NO_2 values whereas model 6 explains 74% of such variation. Thus, it can be concluded that the contribution of road traffic in average NO_2 value is around 75-80% in Jaipur city. To further compare these models, a posterior model probability (p_m) is defined, as given in eqn. 9.

$$p_m = \frac{e^{-0.5\Delta_m}}{\sum_{j=1}^{m} e^{-0.5\Delta_j}} \quad (9)$$

here

$$\Delta_m = AIC_m - AIC_{min}$$

AIC_m: AIC value for model m;

AIC_{min}: the minimum AIC values of all models.

Table 5 also shows the values of posterior model probability of all the models considering the two streams separately and considering only the 5 best models per stream. As can be seen, model 1 has about 42.6% probability of being the best amongst the first five models of stream 1 whereas model 6 has a 39.7% probability of being the best amongst the first five models of stream 2.

As a next step, models 1 and 6 are further analyzed to compare them against each other. Fig. 9 shows the scatter plot between NO_2 and RD_{L1}^{SR750} and $\log_{10}$ variant of the same parameters. As can be seen from the graphs there is a trend in both the curves, however, the range of values is considerably lower in model 6 as compared to model 1.

In model 1, coefficients for RD_{L1}^{SR750}, RD_{L2}^{SR750} and RD_{L3}^{SR750} are calculated as 7.10, 2.52, and -0.58 respectively, and the intercept is 15.07. Similarly, the coefficient for model 6 are 0.45, 0.23, and -0.31 respectively for $\log_{10}$ values of RD_{L1}^{SR750}, RD_{L2}^{SR750} and RD_{L3}^{SR750} and the intercept is 1.57.

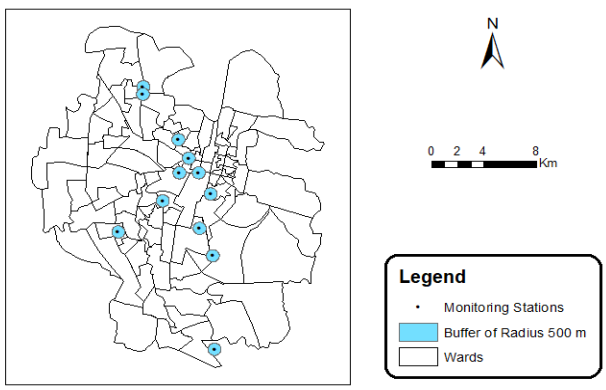

Fig. 9: Buffers around monitoring stations of radius 500 m.

Fig. 10 (a) and (b) shows the graphs between the observed and computed values of NO_2 for model 1 and 6, respectively.

To compare these models for observed values at other cities, two CAAQMS stations of Kota and Jodhpur cities are used. Road maps were prepared in the vicinities of these stations and road density values for levels 1, 2, and 3 roads with a search radius of 750 m were determined. Table 6 below gives details of observed NO_2 values for the year 2019 as well as road density values of different levels for a search radius of 750 m.

Both the cities are also shown in Fig. 10 (a) and (b). It can be seen that model no. 6 poorly estimates the value for Kota city. For Jodhpur city, both models 1 and 6 give similar estimates. Therefore, it is concluded that model 1 is better suited to estimate the value of NO_2 as compared to other models. Therefore, the estimated value of NO_2 values of any area such as wards, roads, plots, or points could be computed by first obtaining road density values of different levels 1, 2, and 3 of the roads at a search radius of 750 m and then using the eqn. 10 below

$$NO_2 = 15.07 + 7.10\, RD_{L1}^{SR750} + 2.52\, RD_{L2}^{SR750} - 0.58\, RD_{L3}^{SR750} \quad (10)$$

Estimated values of NO_2 have been calculated for all the wards of Jaipur city and the map is shown in Fig. 11. This map is very different from that of Fig. 6, which was developed based on interpolated values of NO_2 and then calculating average value over different wards. Also, it can be seen that wards with NO_2 values of more than 35 are more in Fig. 11 as compared to in Fig. 6. Overall it can be concluded that NO_2 values derived from model 1 give a better estimate for the area which is farther away from the air monitoring station as compared to interpolated maps.

CONCLUSION

A new methodology is developed to estimate the level of air pollution parameter NO_2, which is mostly caused by vehicular pollution, by using road density levels of different levels of road network in Jaipur city. The road network of Jaipur city is developed for 3 different levels of roads and

Table 6: Parameters for other cities.

City	NO_2	Road Density for Search Radius of 750 m		
		Level 1	Level 2	Level 3
Kota	29.29	2.068	0.404	16.642
Jodhpur	29.25	1.774	1.513	17.16

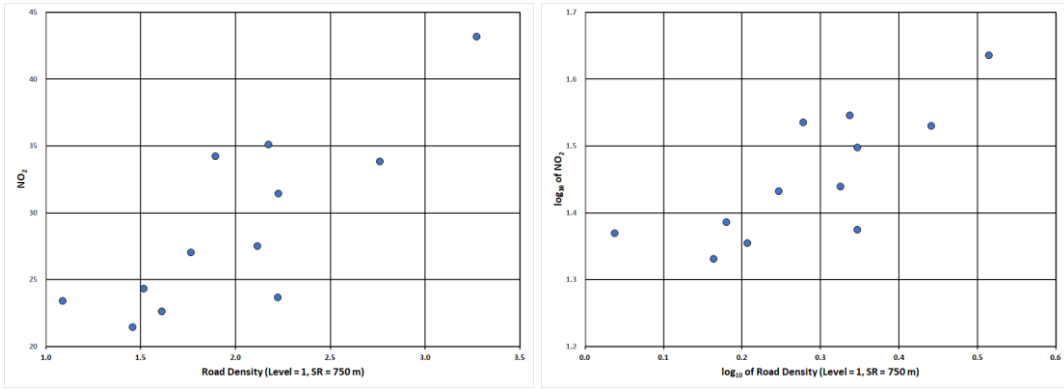

(a) (b)

Fig. 10: (a) Scatter plot between NO_2 and RD_{L1}^{SR750} (b) between log10 values.

road density values are determined in the proximity of air pollution monitoring stations of Jaipur city. Proximity is defined in terms of search radius for measuring road density and buffer distance for air pollution monitoring stations.

It is found that for Jaipur city, linear regression model between measured average NO_2 values of 2019 and road density for search radius and buffer of 750 m is found to best-fitted model. Models are compared based on adj r^2 and AIC values and posterior model probability of the best five models in different streams are determined.

It is found that road networks could explain about 75-80% of the variations in NO_2 values. Also, the finally selected model has a 42.6% probability of being the best model amongst the first five selected from the normal stream of models.

Finally, the selected model is used to calculate estimated values of NO_2 at 91 wards of Jaipur city based on the road network of these wards and this map is compared with another map generated based on interpolated values of NO_2. It is concluded that the map generated from the selected model better explains the spatial distribution of NO_2. This model could also be used in other urban areas where either very few numbers or none at all air pollution monitoring stations are available.

REFERENCES

Analytics Vidya 2020. Key Difference between R-squared and Adjusted R-squared for Regression Analysis. https://www.analyticsvidhya.com/blog/2020/07/difference-between-r-squared-and-adjusted-r-squared/

Arc Map 2020a. Buffer. https://desktop.arcgis.com/en/arcmap/10.3/tools/analysis-toolbox/buffer.htm

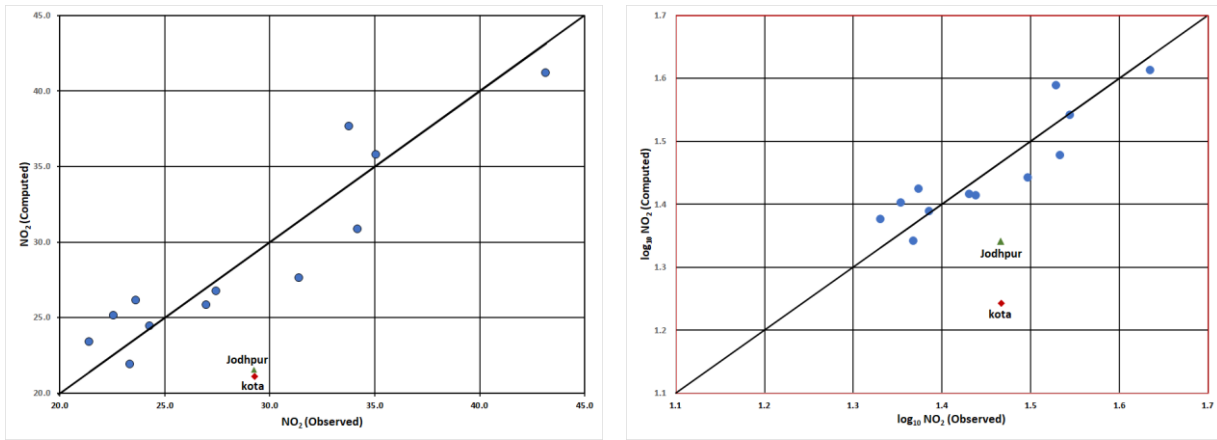

(a) (b)

Fig. 11: Estimated values of NO_2 for different wards.

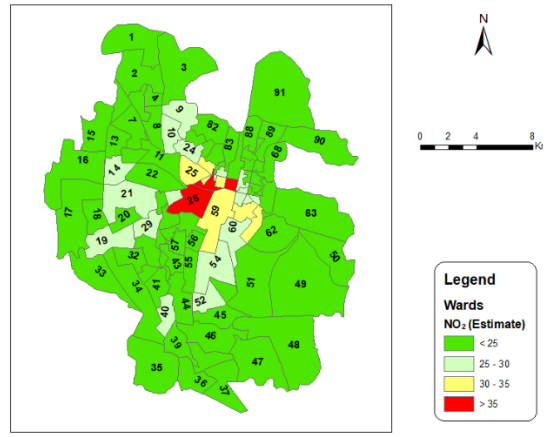

Fig. 12: Observed Vs Computed, (a) Model 1 (b) Model 6.

Arc Map 2020b. Line Density, Arc GIS for Desktop, ESRI, https://desktop.arcgis.com/en/arcmap/10.3/tools/spatial-analyst-toolbox/line-density.htm

Balakrishnan, K., Dey, S. and Gupta, T. 2019. The impact of air pollution on deaths, disease burden, and life expectancy across the states of India: The global burden of disease study 2017. The Lancet: Planet. Health, 3(1): E26-E39

Bechle, J.M., Millet, D.B. and Marshall, J.D. 2013. Remote sensing of exposure to NO2: Satellite versus ground-based measurement in a large urban area. Atmos. Environ., 69: 345-353.

Carslaw, D.C., Farren, N.J., Vaughan, R.V., Drysdale, S.W., Young, S. and James D.L. 2019. The diminishing importance of nitrogen dioxide emissions from road vehicle exhaust. Atmos. Environ., 21: 100002.

CDC. 2019. Air Quality. Centre for Disease Control and Prevention, U.S. Department of Health & Human Services. https://www.cdc.gov/air/pollutants.htm

Costabile, F., Giuliano, B., Santis, D., Bellagotti, F., Ciuchini, R., Vichi, C. and Allegrini, F. I. 2010. Spatial distribution of urban air pollution in Lanzhou, China. Open Environ. Pollut. Toxicol. J., 2: 8-15.

Cowie, C.T., Ding, D. and Rolfe, M.I. 2016. Neighborhood walkability, road density, and socioeconomic status in Sydney, Australia. Environ. Health, 15: 58.

Dadhich, A.P., Goyal, R. and Dadhich, P.N. 2018b. Assessment of spatio-temporal variations in the air quality of Jaipur city, Rajasthan, India. Egypt. J. Remote. Sens. Space Sci., 21(2): 173-181

Dadhich, A.P., Dadhich, P.N. and Goyal, R. (2018a). A GIS-based approach for assessment of ambient air quality in Kota City. J. Basic Appl. Eng. Res., 5(2): 89-93.

EPA. 2016. Nitrogen Dioxide (NO2) Pollution. United States Environmental Protection Agency. https://www.epa.gov/no2-pollution/basic-information-about-no2

Filonchyk, M. and Hurynovich, V. 2020. Spatial distribution and temporal variation of atmospheric pollution in the South Gobi Desert, China, during 2016–2019. Environ. Sci. Pollut. Res., 27**:** 26579–26593.

Health Effects Institute. 2020a. State of Global Air 2020. Global Burden of Disease Study 2019, IHME

Health Effects Institute. 2020b. State of Global Air 2020. Global Burden of Disease Study 2019, IHME.

IASS. 2020. Air Pollution and Climate Change. Institute for Advanced Sustainability Studies. Federal Ministry of Education and Research. https://www.iass-potsdam.de/en/output/dossiers/air-pollution-and-climate-change. Accessed July 2020.

JDA. 2020. Master Development Plan 2025, Jaipur. Urban Development and Housing, Government of Rajasthan.

Khaniabadi, O.Y., Goudarzi, G., Daryanoosh, S.M., Borgini, A., Tittarelli, A. and De Marco, A. 2020. Exposure to PM10, NO2, and O3 and impacts on human health Environ. Sci. Pollut. Res. Int., 24(3): 2781-2789.

Mohammad, A. A. and Juahir, A. (2015). Spatial analysis of certain air pollutants using environmetric techniques. J. Tech., 75: 241-249.

Munoth, M., Tiwari, M. and Goyal, R. (2015). Fluoride and Nitrate Groundwater Contamination in Rajasthan, India: A Review, Hydro 2015 International IIT Roorkee, India, 17-19 December 2015, 20th International Conference on Hydraulics, Water Resources and River Engineering.

Nieto, P.J.G., Antón, J.C.Á. and Vilán, J.A.V. (2015). Air quality modeling in the Oviedo urban area (NW Spain) by using multivariate adaptive regression splines. Environ. Sci. Pollut. Res., **22:** 6642–6659.

ORGCC. 2020. India Annual Health Survey 2012 - 13 Fact Sheet. https://www.censusindia.gov.in/ vital_statistics/AHSBulletins/AHS_Factsheets_2012-13/FACTSHEET-Rajasthan.pdf.

Poeter, E.P. and Anderson, D. 2005. Multimodel ranking and inference in groundwater modeling. Ground Water, 43(4): 597-605.

Rajput, H., Goyal, R. and Brighu, U. 2020. Modification and optimization of DRASTIC model for groundwater vulnerability and contamination risk assessment for Bhiwadi region of Rajasthan, India. Environ. Earth Sci., 79: 136.

Ryu, J., Park, C. and Jeon, S.W. 2019. Mapping and statistical analysis of no2 concentration for local government air quality regulation. Sustainability, 11: 38-49

Singh, V. 2019. Deaths due to air pollution highest in Rajasthan: Experts "Outlook, The News Scroll. https://www.outlookindia.com/newsscroll/deaths-due-to-air-pollution-highest-in-rajasthan-experts/1592817.

Sogani, M. and Vyas, A.D. 2019. Socioeconomic Spillovers Resulting from the Functioning of Sewage Treatment Plants in Jaipur, India: A Case Study of the Delawas Plant. In Yoshino, N., Araral, E. and Seetharam, K.E. (eds.), Water insecurity and sanitation in Asia, Asian Development Bank Institute, Tokyo, Japan, pp. 83-106.

The Hindu. 2015. NO2 Emission Rising in India, New NASA Air Quality Maps Show. https://www.thehindu.com/sci-tech/energy-and-environment/no2-emission-rising-in-india-new-nasa-air-quality-maps-show/article7992190.ece

TNN. 2017. Rajasthan Has the Highest Deaths Due to Chronic Pulmonary Diseases in the Country. The Times of India. https://timesofindia.indiatimes.com/city/jaipur/raj-has-highest-deaths-due-to-chronic-pulmonary-diseases-in-country/articleshow/61652510.cms

UNICEF. 2016 Pollution: 300 million children breathing toxic air - UNICEF report. UNICEF Press release 31 st October 2016.

United States Environmental Protection Agency. 2016. Nitrogen Dioxide (NO2), EPA. The United States Environmental Protection Agency, September 08, 2016

United States Environmental Protection Agency. 2020. Particulate Matter (PM) Pollution, EPA. The United States Environmental Protection Agency, April 13, 2020

Vyas, A D., Mahale, K., Ajmera, D. and Goyal, R. 2020. Optimum weights of environmental parameters in evaluating urban environmental sustainability index: A case study of Jaipur city. ISH J. Hydraulic Eng., 28: 143-156

World Health Organization. 2019. WHO, Health Topics, Air Pollution Overview. www.who.int/2019

Zhou, Y. and Herath, H.M.P.S.D. 2017. Evaluation of alternative conceptual models for groundwater modeling. Geosci. Frontiers, 8: 437-443.

Zhu, Y. and Lok, C.K. 2018. Analysis of spatial and temporal patterns of on-road NO2 concentrations in Hong Kong. Atmos. Meas. Tech., 11: 6719-6734.